

# Rotating electrohydrodynamic flow in a suspended liquid film

E. V. Shiryayeva\* and M. Yu. Zhukov†

*Department of Mathematics, Mechanics and Computer Science,  
Southern Federal University, 344090, Rostov-on-Don, Russia*

V. A. Vladimirov‡

*Department of Mathematics, York University, York, YO10 5DD, UK*

(Dated: October 29, 2018)

The mathematical model of a rotating electrohydrodynamic flow in a thin suspended liquid film is proposed and studied. The motion is driven by the given difference of potentials in one direction and constant external electrical field  $\mathbf{E}_{\text{out}}$  in another direction in the plane of a film. To derive the model we employ the spatial averaging over the normal coordinate to a film that leads to the average Reynolds stress that is proportional to  $|\mathbf{E}_{\text{out}}|^3$ . This stress generates tangential velocity in the vicinity of the edges of a film that, in turn, causes the rotational motion of a liquid. The proposed model is aimed to explain the experimental observations of the *liquid film motor* [1, 2].

PACS numbers: 47.32.Ef, 68.15.+e, 47.57.jd

Keywords: electrohydrodynamic flow, thin film, spatial average

## I. INTRODUCTION

The paper is devoted to the theoretical study of the motions in a thin suspended liquid film. The motions are driven by the constant external electric field that is applied at the edges of a film. We show that this field produces the averaged rotating motion of the liquid in the plane of a film. Our aim is to explain the rotating flow observed in an electrolyze planar water cell placed inside a plane capacitor [1, 2]. The rotating motion of a fluid as a whole caused by the action of a *constant* electrical field is so unusual that the authors of [1, 2] call this effect a *liquid film motor*, emphasizing that it represents a new type of engine. They also proposed that it could be explained by the changing of orientation of water molecular dipoles caused by a strong electric field. Simultaneously they denied the possibility of the generating of such a flow by the edge effects. In contrast, we show that the jump of an electric field across a water-dielectric interface produces the tangential velocity of a liquid that can maintain a steady rotating flow in the whole film. In other words, we demonstrate that one does not need to use a heuristic idea about the switching of the molecular orientations: this phenomenon can be explained with the use of classical tools only. In our model the rotating motion in a film is explained by the electro-kinetic effects at its edges. According to our theory the ratio between the spatial scales of a flow domain plays a crucial role. Only for thin films the classical edge effects can generate the rotation; in contrast in the flow domains with all spatial scales of the same order this effect will be absent. Naturally, our final model is two-dimensional (plane); how-

ever the tangential velocity at the boundary is actually caused by Reynolds stresses that appear after the averaging over a film thickness of an original three-dimensional flow. The resulting tangential velocity has order  $O(h^4)$ , where  $2h$  is a film thickness. An intense electrohydrodynamic (EHD) rotating flow takes place only in the restricted domain of governing parameters. In particular, such a flow can exist for the films of moderate thickness (for example, the tangential velocity  $\sim 1$  cm/sec appears for the following parameters: the strength of the capacitor electric field  $\sim 30$  kV/m, the difference of electrolysis potentials  $\sim 20$  V, the film thickness  $\sim 0.1$ – $0.3$  cm, and the film surface size  $\sim 1$  cm), but it can not exist for very thin films. An important general result of our paper is the demonstration of the fact that the classical effects (such as the electrokinetic phenomena), that are small in ordinary conditions, can play the key part in micro-scales. Such reevaluation of the classical effects may be important for the developments of microfluidics and for the creation of microdevices. Here one have take into account that in this paper we both present systematical theoretical results and show their good agreement with the experiments of [1, 2]. The detailed discussion of our results is given in Sect. VII.

In the mathematical modelling we essentially use the results [3, 4, 5, 6, 7, 8] that contain the analytical and numerical studies of EHD flows with the gradient of conductivity, the method of depth-average, and an effective asymptotic procedure for the EHD equations of multi-component mixtures. In the averaged equations derived in [3, 4, 5, 6, 7] one can see the terms correspondent to Taylor-Aris dispersion and to Reynolds stresses; however Reynolds stresses are neglected since they are small for the chosen intervals of parameters and negligible for the studied phenomena. It is also important that in [6] one can find the comparison between the results for the mathematical models of the different levels of approximation. The papers, closely related to our studies,

---

\*Electronic address: shir@ns.math.rsu.ru

†Electronic address: zhuk@ns.math.rsu.ru

‡Electronic address: vv500@york.ac.uk

[9, 10, 11, 12, 13] consider EHD flows in thin liquid films or in liquid layers with interfaces; paper [14] describes the appearance of vortex rings due to reactions near an electrode; and [15] presents a rotating EHD flow in a smectic medium. The role of interface boundary conditions in the electrohydrodynamics (EHD) is well-known from the classical papers [16, 17, 18]. The paper [19] shows that an electrical double layer (EDL) can allow a slip in the boundary conditions between a liquid and a solid. The papers [20, 21, 22, 23, 24, 25] are devoted to the influence of the inhomogeneous electrical charge of microchannel boundaries on EHD flows. Other closely related papers [26, 27, 28, 29, 30] consider various theories of the EDL, including so-called extremal regimes. The survey of modern EDL-theories can be found in [31].

The interest in various flows of micro- and nano-scales has increased greatly during the last few years. For example, the main parts of the surveys [32, 33] are devoted to EHD processes in microchannels; [34, 35, 36, 37, 38, 39] deal with the injection of a fluid and other flows in microchannels. This interest is strongly stimulated by the creation of the microfabricated fluid devices for the effective separation or the micromixing of multicomponent mixtures [40, 41, 42, 43, 44, 45], the electro-micro-pumps [46], *etc.* These new techniques are known as parts of the *Lab-on-a-Chip technology*. The mathematical models in this research area help to understand and to describe micro-processes, to develop experimental methods, and to construct microchips.

## II. BASIC EQUATIONS

The rectangular thin liquid film with the fixed plane free surfaces  $z = \pm h$  is considered in Cartesian coordinates  $(x, y, z)$  (Fig. 1). The electrical field can be conveniently split into two parts. The first one is due to the constant electric potentials  $\varphi = 0$  and  $\varphi = \varphi_0$  on the boundaries  $x = 0$  and  $x = X$ , so the constant difference of potentials is applied in the direction  $x$ . The second part is the constant external electric field  $\mathbf{E}_{\text{out}}$  that is prescribed at the boundaries  $y = 0$  and  $y = Y$ . The vector  $\mathbf{E}_{\text{out}}$  lies in the plane  $z = \text{const}$ ,  $\alpha$  is the angle between this vector and  $y$ -axis.

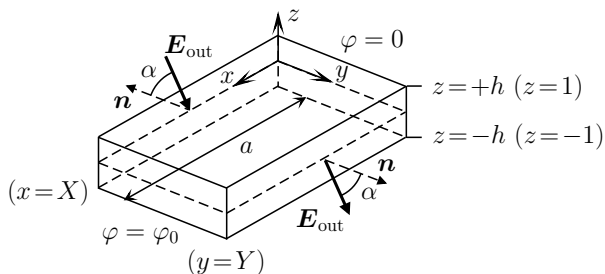


FIG. 1: A thin film. Dimensionless variables are given in parentheses.

We assume that the electric field is potential, the gravity and the surface tension are absent; the dielectric permittivity  $\varepsilon = \text{const}$  that leads to the absence of the ponderomotive force  $(1/2)\nabla\varepsilon(\nabla\varphi)^2 = 0$ . The dimensionless system of governing equations that describes EHD flows of a multicomponent fluid (for example, water with the ions  $\text{H}^+$ ,  $\text{OH}^-$ ) is:

$$\delta^2 \frac{d\mathbf{u}}{dt} = -\delta^2 \nabla_0 p + \delta^2 \nu \Delta_0 \mathbf{u} + \nu \partial_{zz} \mathbf{u} - q \nabla_0 \varphi, \quad (1)$$

$$\delta^4 \frac{dw}{dt} = -\delta^2 \partial_z p + \delta^4 \nu \Delta_0 w + \nu \delta^2 \partial_{zz} w - q \partial_z \varphi, \quad (2)$$

$$\text{div}_0 \mathbf{u} + \partial_z w = 0, \quad (3)$$

$$\varepsilon (\delta^2 \Delta_0 \varphi + \partial_{zz} \varphi) = -\delta^2 q, \quad q = \sum_k e_k c_k, \quad (4)$$

$$\delta^2 \frac{dc_k}{dt} + \delta^2 \text{div}_0 \mathbf{i}_k + \partial_z I_k = 0, \quad (5)$$

$$\mathbf{i}_k = -D_k (\nabla_0 c_k + e_k \gamma c_k \nabla_0 \varphi), \quad (6)$$

$$I_k = -D_k (\partial_z c_k + e_k \gamma c_k \partial_z \varphi),$$

$$\mathbf{\Gamma} = (\sigma_{13}, \sigma_{23}, 0) = \nu (\partial_z \mathbf{u} + \delta^2 \nabla_0 w), \quad (7)$$

$$\frac{d}{dt} = \partial_t + \mathbf{u} \cdot \nabla_0 + w \partial_z, \quad \nabla_0 = (\partial_x, \partial_y), \quad \Delta_0 = \partial_{xx} + \partial_{yy},$$

Here  $\mathbf{v} = (\mathbf{u}, w)$  and  $\mathbf{u} = (u, v)$  is velocity and its  $(x, y)$ -projection,  $p$  is pressure;  $q$  is the density of molar charge;  $\varphi$  is electric potential;  $c_k$  is the molar concentration for the  $k$ -th component of mixture;  $\mathbf{i}_k$  and  $I_k$  are the planar and transversal density fluxes for the concentrations;  $\nu$  is kinematic viscosity;  $D_k$  is the diffusivity for the components of mixture;  $e_k$  are the electric charges of components (in the units of electron's charge);  $\varepsilon$  is the solution permittivity; the parameter  $\gamma$  characterises the ratio between the transports of concentrations by the electrical field and by diffusion;  $2\delta$  is a dimensionless film thickness;  $\mathbf{\Gamma}$  is the tangential stress vector that is expressed via the components  $\sigma_{13}$ ,  $\sigma_{23}$  of a viscous stress tensor.

On the film boundaries  $z = \pm 1$  we accept: the no-leak condition for velocity

$$w|_{z=\pm 1} = 0, \quad (8)$$

the stress-free condition, that with the use of (8) is

$$\mathbf{\Gamma}|_{z=\pm 1} = \nu (\partial_z \mathbf{u} + \delta^2 \nabla_0 w)|_{z=\pm 1} = \nu \partial_z \mathbf{u}|_{z=\pm 1} = 0, \quad (9)$$

the no-leak conditions for concentrations

$$I_k|_{z=\pm 1} = 0 \quad (10)$$

and the vanishing of the normal electrical current

$$\partial_z \varphi|_{z=\pm 1} = 0. \quad (11)$$

We use the governing equations (1)–(7) for the deriving of the averaged model in Sect. III and in Appendix A. In our averaging procedure we use only the boundary conditions (8)–(11). The other boundary conditions (defined for the averaged equations) are given in Sect. III.

For the introducing of dimensionless variables we use the following characteristic values of parameters:

$$\begin{aligned} [x, y] &= a, & [z] &= h, & [t] &= \mathcal{T}, & [u, v] &= \frac{a}{\mathcal{T}}, & [w] &= \frac{h}{\mathcal{T}}, \\ [c_k] &= C, & [E] &= \mathcal{E}, & [\varphi] &= \mathcal{E}a, & [q] &= FC, & \gamma &= \frac{F\mathcal{E}a}{RT}, \\ [p] &= FC\mathcal{E}a\delta^2, & \mathcal{T}^2 &= \frac{\rho a}{FC\mathcal{E}\delta^2}, & \delta^2 &= \frac{h^2}{a^2}. \end{aligned} \quad (12)$$

Here  $a$  is the characteristic length in the plane of the film;  $h$  and  $\delta$  are the dimensional and dimensionless half-thickness of the film;  $\rho$  is the density of a liquid;  $\mathcal{T}$ ,  $\mathcal{P}$ ,  $C$  are characteristic time, pressure, and molar concentration;  $FC$  is characteristic charge density;  $F$  is Faraday constant;  $R$  is the universal gas constant;  $T$  is the absolute temperature of solution;  $a\mathcal{E}$  is the characteristic difference of electric potentials in the  $x$ -direction. The dimensional values of kinematic viscosity  $\nu^*$ , diffusion coefficients  $D_k^*$ , and the dielectric permittivity  $\varepsilon^*$  are linked to their dimensionless counterparts as:

$$\nu = \frac{\nu^*\mathcal{T}}{a^2}, \quad D_k = \frac{D_k^*\mathcal{T}}{a^2}, \quad \varepsilon = \frac{\varepsilon^*\mathcal{E}}{aFC}. \quad (13)$$

The use of dimensionless parameters (viscosity, diffusivity, *etc.*) instead of conventional scaling numbers (Reynolds number, Peclet number, *etc.*) is more convenient for our purposes since they allow us to see what physical effects participate into a certain process. The connections between the introduced parameters and the scaling numbers are apparent:

$$\text{Re} = \frac{1}{\nu}, \quad \text{Pe}_k = \frac{1}{D_k}.$$

### III. THE AVERAGING ACROSS A FILM

The main part of the employed averaging procedure is the same as in [3, 4, 5, 6, 7]. The operation of averaging is defined as:

$$\bar{f}(x, y, t) = \frac{1}{2} \int_{-1}^1 f(x, y, z, t) dz, \quad \tilde{f} \equiv f - \bar{f}. \quad (14)$$

We decompose the solution of (1)–(11) into the series

$$\begin{aligned} \{\mathbf{u}, w, p, q, c_k, \varphi\} &= \sum_{m=0} \{\mathbf{u}^m, w^m, p^m, q^m, c_k^m, \varphi^m\} \delta^{2m} = \\ &= \sum_{m=0} \{\bar{\mathbf{u}}^m, \bar{w}^m, \bar{p}^m, \bar{q}^m, \bar{c}_k^m, \bar{\varphi}^m\} \delta^{2m} + \\ &+ \sum_{m=0} \{\tilde{\mathbf{u}}^m, \tilde{w}^m, \tilde{p}^m, \tilde{q}^m, \tilde{c}_k^m, \tilde{\varphi}^m\} \delta^{2m}. \end{aligned} \quad (15)$$

The averaging of the governing equations (1)–(6), which takes into account the boundary conditions (8)–(11) and the decomposition in small parameter  $\delta^2$ , first yields  $\bar{q} = \bar{q}^0 + O(\delta^2)$ ,  $\bar{\varphi} = \bar{\varphi}^0 + O(\delta^2)$ ,  $\bar{c}_k = \bar{c}_k^0 + O(\delta^2)$ ,  $\tilde{\varphi}^0 = 0$ ,  $\tilde{c}_k^0 = 0$ ,  $\tilde{q}^0 = 0$  and then leads to the expressions for  $\tilde{\mathbf{u}}^0$ ,  $\tilde{w}^0$ ,  $\tilde{c}_k^1$ . The averaged plane equations which keep the terms  $O(\delta^2)$  are (for the details see Appendix A)

$$\delta^2 \frac{d_0 \bar{\mathbf{u}}}{dt} + \beta \nabla_0 (\mathbf{U} \otimes \mathbf{U}) = -\delta^2 \nabla_0 \bar{p} + \delta^2 \nu \Delta_0 \bar{\mathbf{u}} - \nu \mathbf{U}, \quad (16)$$

$$\text{div}_0 \bar{\mathbf{u}} = 0, \quad (17)$$

$$\varepsilon \Delta_0 \bar{\varphi} = -\bar{q}, \quad \bar{q} = \sum_k e_k \bar{c}_k, \quad (18)$$

$$\frac{d_0 \bar{c}_k}{dt} - \alpha_k \delta^2 \text{div}_0 (\mathbf{U} (\mathbf{U} \cdot \nabla_0 \bar{c}_k)) + \text{div}_0 \bar{\mathbf{i}}_k = 0, \quad (19)$$

$$\bar{\mathbf{i}}_k = -D_k (\nabla_0 \bar{c}_k + e_k \gamma \bar{c}_k \nabla_0 \bar{\varphi}),$$

$$\frac{d_0}{dt} = \partial_t + \bar{\mathbf{u}} \cdot \nabla_0, \quad \nu \mathbf{U} = \bar{q} \nabla_0 \bar{\varphi}, \quad (20)$$

$$\beta = \frac{\delta^2}{45}, \quad \alpha_k = \frac{4}{945 D_k},$$

where  $(\mathbf{U} \otimes \mathbf{U})$  denotes a tensorial product. We emphasize that after this averaging  $\delta$  must be treated as a regular independent parameter of the problem, together with  $\nu$ ,  $\varepsilon$ ,  $D_k$ , *etc.*

For the equations (16)–(20) we prescribe the boundary conditions for the averaged fields  $\bar{\mathbf{u}}$ ,  $\bar{c}_k$ ,  $\bar{\varphi}$  on the side boundaries  $x = 0, X$  and  $y = 0, Y$  (Fig. 1).

The boundaries  $y = 0$  and  $y = Y$  represent the interfaces between two dielectric materials: the liquid with the dielectric permittivity  $\varepsilon$  and the outside medium with the dielectric permittivity  $\varepsilon_{\text{out}}$ ; these boundaries are insulators (not electrodes), hence we prescribe the continuity of the normal components for electrical induction [47, 48]

$$\varepsilon (\mathbf{n} \cdot \nabla_0 \bar{\varphi}) = \varepsilon_{\text{out}} (\mathbf{n} \cdot \mathbf{E}_{\text{out}}), \quad y = 0, Y,$$

where  $\mathbf{n}$  is the unit normal vector to the boundary. Since the vector  $\mathbf{E}_{\text{out}}$  lies in the plane  $z = \text{const}$  and has the angle  $\alpha$  with  $y$ -axis we have

$$\frac{\partial \bar{\varphi}}{\partial \mathbf{n}} = \pm E_0, \quad y = 0, Y; \quad E_0 = \frac{\varepsilon_{\text{out}}}{\varepsilon} |\mathbf{E}_{\text{out}}| \cos \alpha, \quad (21)$$

where the sign ‘-’ corresponds to the boundary  $y = 0$  (Fig. 1) [53]. The conditions of zero concentration fluxes at  $y = 0, Y$  are

$$\bar{\mathbf{i}}_k \cdot \mathbf{n} = 0, \quad y = 0, Y. \quad (22)$$

The fixed difference between the electric potentials at  $x = 0, x = X$  is given as

$$\bar{\varphi} = 0, \quad x = 0; \quad \bar{\varphi} = \varphi_0, \quad x = X. \quad (23)$$

For all edge boundaries  $x = 0, X$  and  $y = 0, Y$  we require the no-leak of a liquid

$$\bar{\mathbf{u}}|_{x=0, X} = 0, \quad \bar{\mathbf{v}}|_{y=0, Y} = 0 \quad (24)$$

and the conditions

$$\bar{\mathbf{u}} \cdot \boldsymbol{\tau}|_{y=0, Y} = -\mathcal{R} \nabla_0 \bar{\varphi} \cdot \boldsymbol{\tau}|_{y=0, Y}, \quad (25)$$

$$\bar{\mathbf{u}} \cdot \boldsymbol{\tau}|_{x=0, X} = -\mathcal{R} \nabla_0 \bar{\varphi} \cdot \boldsymbol{\tau}|_{x=0, X}, \quad (26)$$

where  $\boldsymbol{\tau}$  is a unit tangent vector to the boundary,  $\mathcal{R}$  is the coefficient defined in Sect. IV. By virtue of (23) the boundary conditions (26) for  $x = 0, X$  take the form of no-slip condition

$$\bar{\mathbf{v}}|_{x=0, X} = 0. \quad (27)$$

The prescription of the tangential velocity (25) at the boundaries  $y = 0, Y$  is justified in Sect. IV where we derive it and show that  $\mathcal{R} \sim E_0^3$ . It is derived from the equation (16) that contains the averaged Reynolds stresses

$$\beta \nabla_0 (\mathbf{U} \otimes \mathbf{U}) \equiv \beta (\mathbf{U} \cdot \nabla_0 \mathbf{U} + \mathbf{U} \operatorname{div}_0 \mathbf{U}), \quad (28)$$

which define  $\mathcal{R}$  for certain intervals of parameters  $\nu, \delta, \epsilon, \text{ etc.}$

The derivation of (16)–(20) is given in Appendix A, here we mention only that the boundary conditions (8)–(11) at  $z = \pm 1$  play a central part in this derivation. It is also well-known that if we use only spatial averaging it does not allow us to produce the closed systems of equations; for its closure one has to employ some additional hypothesis. As such a hypothesis we propose the condition  $\bar{\mathbf{w}}^0 = 0$  that is physically natural and accepted without any mathematical justification. The equations similar to (16)–(20) have been obtained in [3, 4, 5, 6, 7] (and other papers cited there) devoted to the studies of EHD flows with the spatially nonuniform conductivity in the microchannels with solid boundaries. These papers also contain the decomposition into the power series and even the term similar to (28). However the key difference with our paper is: for the physical parameters considered in [3, 4, 5, 6, 7] this term is small, so it is naturally neglected.

#### IV. THE FLOWS NEAR BOUNDARIES

The problem (16)–(28) can be split into the sequence of two problems: (i) the calculation of  $\mathcal{R}$  in (25), and (ii) the finding of the averaged velocity field  $\bar{\mathbf{u}}$  and the potential  $\bar{\varphi}$ . In order to evaluate  $\mathcal{R}$  we assume that the mixture is electroneutral everywhere except the vicinities of the boundaries  $y = 0, Y$ . In these vicinities we build the boundary-layer solution that leads to a good estimation for  $\mathcal{R}$ . The detailed studies of the related double layers (the Gouy-Chapman layer, the Stern layer *etc.*) can be found in [19, 21, 22, 23, 24, 27, 28, 29, 30, 31], where nonlinear and steric effects are taken into account along with the linear electrokinetic effects. From the mathematical viewpoint different EDL theories are aimed to formulate and to justify different boundary conditions for the related boundary layers. The main question is how to choose the mutual positions of a physical boundary and an interface between the regions with positive and negative charges.

Let us consider the vicinity of the boundary  $y = 0$  (the case  $y = Y$  is similar) and look for a steady solution of the problem (16)–(24) neglecting in (19) the terms  $\alpha_k \theta^2 \mathbf{U} (\mathbf{U} \cdot \nabla_0 \bar{c}_k)$

$$\bar{\mathbf{u}} = (\bar{u}(y), 0), \quad \bar{c}_k = \bar{c}_k(y), \quad \bar{\varphi} = \Phi(y) + Ex, \quad (29)$$

where  $E$  is the constant tangential component of the electrical field in the vicinity of  $y = 0$ . The integration of (19) with the boundary conditions (22) yields

$$\bar{c}_k(y) = c_{Bk} e^{-e_k \gamma \Phi(y)}, \quad \bar{q}(y) = \sum_k e_k c_{Bk} e^{-e_k \gamma \Phi(y)}, \quad (30)$$

where  $c_{Bk}$  are the constants representing concentrations for the equilibrium Boltzmann distributions. We restrict ourselves with the case when the mixture is electroneutral, only two kinds of ions are present (for example  $\text{H}^+$  and  $\text{OH}^-$  for water), and the equilibrium Boltzmann distribution is valid:

$$c_{B1} = c_{B2} \stackrel{\text{def}}{=} c_B, \quad z_1 = 1, \quad z_2 = -1. \quad (31)$$

The Poisson-Boltzmann equation (18) takes the form

$$\lambda^2 \partial_{yy} \theta = \sinh \theta, \quad \theta(y) = \gamma \Phi(y). \quad (32)$$

where  $\lambda_D$  (or  $\lambda$ ) are (or relative) Debye’s length:

$$\lambda^2 = \frac{\epsilon}{2\gamma c_B} = \frac{\lambda_D^2}{a^2} \ll 1, \quad \lambda_D^2 = \frac{\epsilon^* RT}{2c_B^* F^2}. \quad (33)$$

In the vicinity of  $y = 0$  the boundary layer variable is introduced as  $y = \lambda \eta$  (similarly, at  $y = Y$  the change of variable is  $y = Y + \lambda \eta$ ). In the more precise terms the considered boundary-layer solution represents so called ‘penetrating boundary layer’ [49]. In this case the original equations and the boundary-layer equations coincide, and  $\lambda \ll 1$  is not required for the obtaining of the solution. Instead of the looking for the boundary-layer solution decaying at infinity one can use the symmetry with

respect to the middle of the domain ( $y = Y/2$ ); the result will remain the same. Nevertheless our further consideration follows the path that is more transparent from the physical viewpoint. The equation (32) takes form

$$\partial_{\eta\eta}\theta(\eta) = \sinh\theta(\eta). \quad (34)$$

Its integration with the boundary condition (21) for  $\Phi(0)$  yields

$$\theta(0) = -\theta_0, \quad \gamma\Phi(0) = -\theta_0 \quad (35)$$

where

$$\theta_0 = \ln\left(1 + \mathbb{E}^2 + \mathbb{E}\sqrt{2 + \mathbb{E}^2}\right), \quad \mathbb{E}^2 = \frac{\gamma\varepsilon}{4c_B}E_0^2,$$

The expression for  $\Phi(Y)$  is similar to (35)

$$\theta(0) = \theta_0, \quad \gamma\Phi(Y) = \theta_0,$$

The boundaries  $y = 0$  and  $y = Y$  represent the different plates of the capacitor, therefore the opposite signs of the potential  $\Phi$  are apparent. The calculation of  $\beta\nabla_0(\mathbf{U}\otimes\mathbf{U})$  with the use of (28), (20), (29) yields

$$\beta\nabla_0(\mathbf{U}\otimes\mathbf{U}) = \frac{\beta}{\nu^2}\left(E\partial_y(\bar{q}^2\partial_y\Phi), \partial_y(\bar{q}\partial_y\Phi)^2\right). \quad (36)$$

where the righthand side (written in components) allows us to integrate the equation (16) with the additional condition  $u(\infty) = 0$ . This condition means that the flow arising near the boundary must decay at large distances, *i.e.* that the distributions of the horizontal component  $u$  and potential  $\Phi$  are of a boundary-layer type (for more details see Appendix B)

$$\frac{\beta E \varepsilon^2}{\nu^2 \lambda^4 \gamma^3} \int_{\infty}^{\eta} (\partial_{\eta\eta}\theta)^2 \partial_{\eta}\theta \, d\eta = \delta^2 \nu u(\eta) + \frac{\varepsilon E \theta(\eta)}{\gamma}. \quad (37)$$

Recall once again that the solutions for  $u$  and  $\Phi$  represent a ‘penetrating boundary layer’, so one can obtain the exact solution with the use of symmetry by taking  $u = 0$  at the middle of the domain ( $y = Y/2$ ). For the obtaining of the boundary condition (25) and defining  $\mathcal{R}$  we evaluate the integral at  $\eta = 0$ :

$$\int_{\infty}^0 (\partial_{\eta\eta}\theta)^2 \partial_{\eta}\theta \, d\eta = \int_0^{\theta(0)} \sinh^2 \theta \, d\theta = \frac{1}{2}(\sinh \theta_0 \cosh \theta_0 - \theta_0).$$

Taking into account that  $E = -(\boldsymbol{\tau}\cdot\nabla_0\varphi)_{y=0}$  and comparing (37) with (25) we obtain (the case  $y = Y$  is similar)

$$\mathcal{R}_3 = \pm \frac{2c_B^2\beta}{\delta^2\nu^3\gamma}(\sinh \theta_0 \cosh \theta_0 - \theta_0), \quad \mathcal{R}_1 = \pm \frac{\varepsilon}{\delta^2\nu\gamma}\theta_0, \quad (38)$$

$$\mathcal{R} = \mathcal{R}_3 + \mathcal{R}_1,$$

where different signs correspond to  $y = 0$  and  $y = Y$ . With a sufficient precision the value of  $\mathcal{R}_3$  at  $\mathbb{E} \leq 1.5$  can be replaced with

$$\mathcal{R}_3 \approx \pm \frac{8c_B^2\beta}{3\delta^2\nu^3\gamma}\sqrt{2}\mathbb{E}^3, \quad \mathbb{E} \leq 1.5. \quad (39)$$

In order to avoid misunderstanding we should mention that the calculated value of  $\mathcal{R}$  (25) represents only a rough estimation; to obtain it we accept that the equation (19) is steady and neglect the Taylor-Aris dispersion. Moreover, in (29) we assume that  $E = \text{const}$  on the boundaries  $y = 0, Y$  that is not true, later on we consider  $E = E(x)$  (see (45)). In spite of these simplifying assumptions, the results of this section show that Reynolds stresses  $\beta\nabla_0(\mathbf{U}\otimes\mathbf{U})$  for certain parameters can crucially participate to the generation of the tangential velocity (of order  $O(E_0^3)$ ) at the side boundary of a film.

## V. THE FLOW IN A THIN FILM

In order to describe the flow in a thin film we use the simplified version of the equations (16)–(20), where we accept that the mixture is electroneutral ( $\bar{q} = 0$ ) everywhere but the vicinities of the boundaries. It allows us to eliminate from the equations all terms proportional to  $\mathbf{U}$ , taking them into account only in the boundary conditions (see Sect. IV). The problem describing the averaged velocity  $\bar{\mathbf{u}} = (\bar{u}, \bar{v})$  and the averaged potential  $\bar{\varphi}$  is

$$\partial_i\bar{\mathbf{u}} + \bar{\mathbf{u}}\cdot\nabla_0\bar{\mathbf{u}} = -\nabla_0\bar{p} + \nu\Delta_0\bar{\mathbf{u}}, \quad \text{div}_0\bar{\mathbf{u}} = 0. \quad (40)$$

$$\Delta_0\bar{\varphi} = 0, \quad (41)$$

where (41) corresponds to the continuity equation for an electric current in the case of constant conductivity and equal diffusion coefficients  $D_k$  (see Appendix C); (41) is not the Poisson-Boltzmann equation (18) that express the potential via the charge that was used in Sect. IV, the formal coincidence of these equations should not cause misunderstanding. We solve (40), (41) in the rectangular domain  $D = \{0 \leq x \leq X, 0 \leq y \leq Y\}$  with the boundary conditions (21), (23), (24), (26), (27)

$$\bar{\mathbf{u}}|_{x=0, X} = 0, \quad \bar{v}|_{y=0, Y} = 0 \quad (42)$$

$$\bar{u}|_{y=0, Y} = -\mathcal{R}\bar{\varphi}_x|_{y=0, Y}, \quad \mathcal{R} = \mathcal{R}_1(E_0) + \mathcal{R}_3(E_0), \quad (43)$$

$$\bar{\varphi}|_{x=0} = 0, \quad \bar{\varphi}|_{x=X} = \varphi_0, \quad \bar{\varphi}_y|_{y=0, Y} = E_0. \quad (44)$$

Recall that the expression for  $\mathcal{R}$  is given by (38), (39) and the value of  $\mathcal{R}$  essentially depends on  $E_0$ .

The problem (41), (44) has an analytic solution that can be presented as Fourier’s series. For the further use

we give only the following formula (where the sign ‘+’ corresponds to  $y = 0$ )

$$\bar{\varphi}_x|_{y=0, Y} = \frac{\varphi_0}{X} \pm E_0 G(x; X, Y), \quad (45)$$

$$G(x; X, Y) = \frac{4}{\pi} \sum_{k=0}^{\infty} \frac{\tanh \frac{(2k+1)\pi Y}{2X}}{(2k+1)} \cos(2k+1) \frac{\pi x}{X}.$$

The computed graphs of  $G(x; X, Y)$  for different values of  $X, Y$  are shown in Fig. 2.

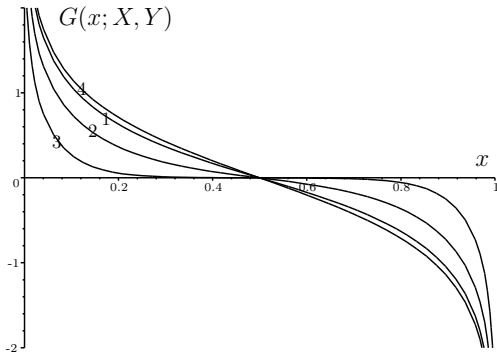


FIG. 2: The function  $G(x; X, Y)$  for  $X = 1$  and the different values of  $Y$ : (1)  $Y = 1$ ; (2)  $Y = 0.5$ ; (3)  $Y = 0.2$ ; and (4)  $Y = 2$

It is apparent that for the fixed  $X, Y$  the sign of  $\bar{\varphi}_x|_{y=0, Y}$  (and hence the tangential velocity  $\bar{u}|_{y=0, Y}$  given by (43)) depends on the relation between the parameters  $\varphi_0, E_0$ . For example, for  $X = Y = 1$  and  $\varphi_0/X = E_0$  the velocity  $u < 0$  on the part of the boundary  $\{0 < x \lesssim 0.1, y = 0\}$ , and  $u > 0$  on the rest of it  $\{0.1 \lesssim x < 1, y = 0\}$ .

## VI. THE NUMERICAL RESULTS

We solve the Navier-Stokes equations (40) with the prescribed tangential velocity and the no-leak condition at  $y = 0, Y$  and the no-slip condition at the rest of the boundary (42), (43) by the employment of the standard projection algorithm [50, 51] and the finite element method. The numerical setting is based on the package FreeFem++ [52] with the use of adaptive grids. The formula (45) for  $\bar{\varphi}_x|_{y=0, Y}$  is not efficient due to its singularities at  $x = 0, X$ ; therefore taking into account the singularities of derivatives near the vertices we also find  $\bar{\varphi}$  (41), (44) numerically.

The formulated problem is rather simple, however the qualitative properties of its solution strongly depend on the relation between the parameters  $\varphi_0, E_0, X, Y$ . As we have already mentioned the direction of the tangential velocity on the boundaries  $y = 0, Y$  is defined by (45) (Fig. 2): the velocity is positive on one part of the boundary and negative on its remaining part (Fig. 3) in

such a way that the particular velocity distribution depends mainly on the ratio  $\varphi_0/E_0$ . It is apparent that this tangential velocity causes the rotational motion of a large scale. Additional smaller vortices can appear in the regions adjacent to the parts of the boundary, where the tangential velocity has the opposite sign (Fig. 3).

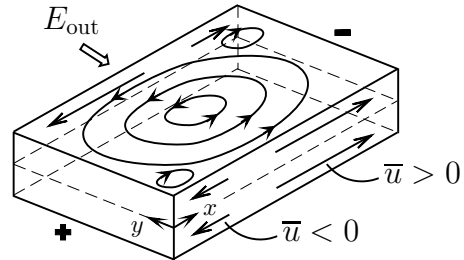


FIG. 3: The sketch of a rotating flow in the film

It is instructive to express dimensionless parameters in terms of dimensional ones with the use of (12), (13), (38), (39)

$$\frac{a}{T} \mathcal{R}_1 = -\frac{\varepsilon^* \mathcal{E}^2}{\rho \nu^*} \lambda_D E_0, \quad (46)$$

$$\frac{a}{T} \mathcal{R}_3 \approx \frac{F c_B^* \varepsilon^* \mathcal{E}^3}{135 \rho^2 \nu^{*3}} \left( \frac{2 \varepsilon^* \mathcal{E}^2}{RT c_B^*} \right)^{1/2} E_0^3 h^4,$$

$$\lambda_D = \left( \frac{\varepsilon^* RT}{2 c_B^* F^2} \right)^{1/2}, \quad \left( \frac{\varepsilon^* \mathcal{E}^2}{4 RT c_B^*} \right)^{1/2} E_0 \leq 1.5.$$

$$\mathcal{T} = \frac{1}{\delta} \sqrt{\frac{\rho a}{FC \mathcal{E}}}, \quad \nu = \frac{\nu^* \mathcal{T}}{a^2}, \quad E_0 = \frac{\varepsilon_{\text{out}}^* E_{\text{out}}^*}{\varepsilon^* \mathcal{E}}, \quad \varphi_0 = \frac{\varphi_0^*}{a \mathcal{E}}.$$

We perform our computations for the experimental values of *parameters for a liquid film motor* taken from [1, 2]; all used values are listed in Tables I, II, III. It is apparent that the velocity  $(a/T) \mathcal{R}_1$  (that is similar to the classic electroosmosis) is significantly less than the tangential velocity on the boundary  $(a/T) \mathcal{R}_3$  that appears due to the averaging over the film thickness. Therefore in the computations we have not taken  $\mathcal{R}_1$  into account.

TABLE I: Dimensional parameters

| Symbol                       | Description              | Value                           |
|------------------------------|--------------------------|---------------------------------|
| $\varphi_0^*$                | difference of potentials | 20 V                            |
| $a$                          | length                   | $10^{-2}$ m                     |
| $E_{\text{out}}^*$           | electric intensity       | 30000 V/m                       |
| $\nu^*$                      | kinematic viscosity      | $10^{-6}$ m <sup>2</sup> /s     |
| $\varepsilon_0^*$            | absolute permittivity    | $8.85 \cdot 10^{-12}$ C/(V · m) |
| $\varepsilon^*$              | water permittivity       | $78.3 \varepsilon_0^*$          |
| $\varepsilon_{\text{out}}^*$ | air permittivity         | $1.0 \varepsilon_0^*$           |
| $\rho$                       | water density            | $10^3$ kg/m <sup>3</sup>        |
| $C = c_B^*$                  | ion concentration        | $10^{-4}$ mol/m <sup>3</sup>    |
| $F$                          | Faraday constant         | $9.65 \cdot 10^4$ C/mol         |
| $R$                          | universal gas constant   | 8.3 J/(mol · K)                 |
| $T$                          | absolute temperature     | 293 K                           |

TABLE II: Characteristic scales

| Symbol                         | Description              | Value                   |
|--------------------------------|--------------------------|-------------------------|
| $\mathcal{E}$                  | electric strengths scale | 2000 V/m                |
| $\mathcal{T}$                  | time scale               | $7.8 \cdot 10^{-2}$ s   |
| $a/\mathcal{T}$                | velocity scale           | 0.128 m/s               |
| $\mathcal{R}_3(a/\mathcal{T})$ | tangent velocity scale   | $3 \cdot 10^{-2}$ m/s   |
| $\mathcal{R}_1(a/\mathcal{T})$ | tangent velocity scale   | $0.5 \cdot 10^{-6}$ m/s |
| $\lambda_D$                    | Debye's length           | $0.95 \cdot 10^{-6}$ m  |
| $h = \delta a$                 | halfheight               | $0.29 \cdot 10^{-2}$ m  |

TABLE III: Dimensionless parameters

| Fig.   | $E_0$ | $\varphi_0$ | $\delta$ | $\nu$               | $\mathcal{R}_3$ | $\mathcal{R}_3/E_0^3$ | $X$ | $Y$ |
|--------|-------|-------------|----------|---------------------|-----------------|-----------------------|-----|-----|
| 4–6, 8 | 0.19  | -1.0        | 0.29     | $7.8 \cdot 10^{-4}$ | 0.235           | 33.42                 | 1.0 | 1.0 |
| 7      | 0.19  | -1.0        | 0.29     | $7.8 \cdot 10^{-4}$ | 0.235           | 33.42                 | 1.0 | 0.5 |
| 9      | 0.19  | -0.1        | 0.29     | $7.8 \cdot 10^{-4}$ | 0.235           | 33.42                 | 1.0 | 1.0 |

One can see that  $\delta^2 \approx 0.09$ ; it gives us a sufficient ground to treat  $\delta^2$  as a small parameter and to use (16)–(20).

The following figures show the results of computations in a square and in a rectangular domain. Fig. 4 shows the isolines for the potential  $\bar{\varphi}(x, y)$  with the step 0.05.

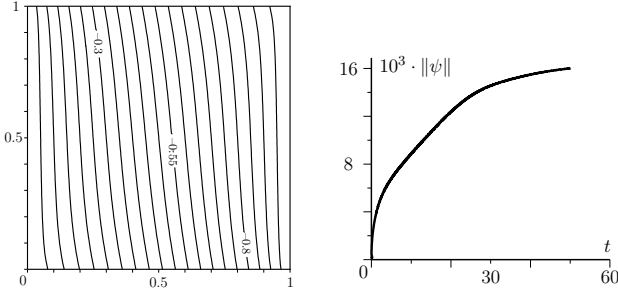
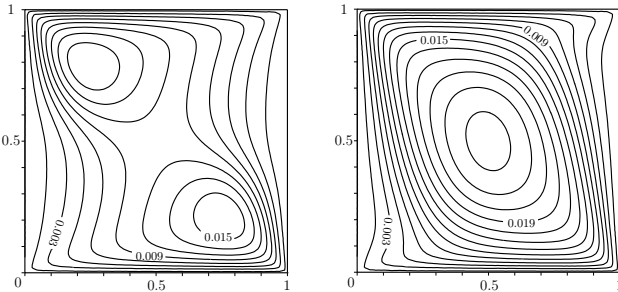
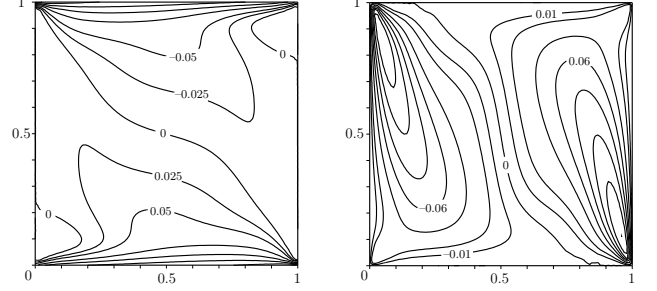
FIG. 4: The isolines of the potential  $\bar{\varphi}(x, y)$  (left) and  $\|\bar{\psi}(\cdot, t)\|$ 

Fig. 5 demonstrates the streamlines of  $\bar{\psi}(x, y, t)$  with the step 0.002 at the instants  $t = 10$  ( $\approx 0.78$  s)  $t = 30$  ( $\approx 2.34$  s).

FIG. 5: The streamlines of  $\bar{\psi}(x, y, t)$  for  $t = 10$  ( $\approx 0.78$  s) and  $t = 30$  ( $\approx 2.34$  s)

The isolines of the velocity field  $\bar{\mathbf{u}}(x, y, t)$  at  $t = 30$  are given in Fig. 6. After  $t = 30$  the flow is practically

steady; for the additional control of the relaxation to a steady state we calculate the mean-square norm  $\|\bar{\psi}(\cdot, t)\|$  (Fig. 4).

FIG. 6: The isolines of  $\bar{\mathbf{u}}(x, y, t)$  (left) and  $\bar{\mathbf{v}}(x, y, t)$  at  $t = 30$ 

More detailed discussion of the computational results is given in Sect. VII. Here we just mention that Fig. 5 shows the initial appearance of two co-rotating vortices. Later on, these two vortices merge into a single vortex that represents an almost steady rotating flow in the whole domain. For the considered parameters the transition (relaxation) to the final steady flow takes around 2 s.

In addition to the computations in a square domain, we perform the computations in rectangular domains with different  $Y$ . In all cases  $X > Y$  we observe a flow structure similar to the shown in Fig. 5: the initial appearance of two vortices with the subsequent forming of an unified steady rotating flow. For example, the flow for  $X = 1, Y = 0.5$  at the instants  $t = 7$  ( $\approx 0.546$  s)  $t = 30$  ( $\approx 2.34$  s) is shown in Fig. 7.

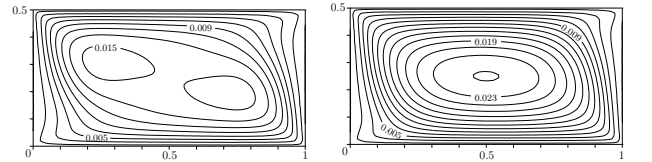
FIG. 7: The streamlines of  $\bar{\psi}(x, y, t)$  for  $X = 1, Y = 0.5$  at  $t = 7$  ( $\approx 0.546$  s) and  $t = 30$  ( $\approx 2.34$  s)

Fig. 8 shows the flows for the square domain with the deliberately smoothed angles (the curvature radius is 0.1). One can see that the singularities in the electrical field near the vertices do not alter the flow structure. In these computations we keep the boundary conditions (42)–(44) at  $x = 0, X$  the same, while on the rest of the boundary we introduce physically similar conditions. In these computations  $\bar{\varphi} = 0$  on the part  $[A, B]$  of the boundary, and  $\bar{\varphi} = \varphi_0$  on  $[C, D]$ . The external electric field acts in the  $y$ -direction. On the rest of the boundary the tangential velocity component is proportional to the tangential derivative of the potential (similar to (43)). We also keep the no-leak condition valid on the whole boundary.

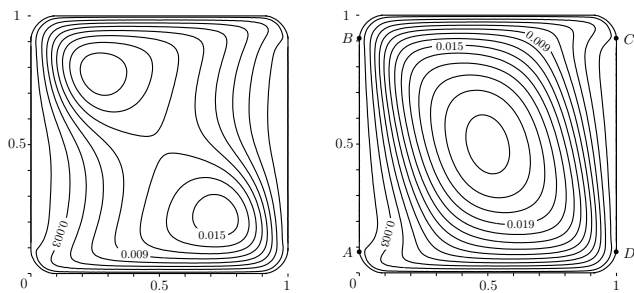


FIG. 8: The streamlines for  $\bar{\psi}(x, y, t)$  at  $t = 10$  ( $\approx 0.78$  s) and  $t = 30$  ( $\approx 2.34$  s)

We have already mentioned that the tangential velocity at the boundary is determined by the relation between the parameters  $\varphi_0$ ,  $E_0$ ,  $X$ ,  $Y$  (see (45)) with one possible flow regime shown in Fig. 3. In order to confirm its existence we present in Fig. 9 the results for the parameters:  $\varphi_0 = -0.1$ ;  $E_0 = 0.19$ ;  $X = 1$ ;  $Y = 1$ . One can see there the isolines of the potential with the step 0.01 and the streamlines at  $t = 200$  with the step 0.0002. The shown flow regime is almost steady: the norm  $\|\bar{\psi}(\cdot, t)\| = 0.001442$  in the interval  $160 < t < 200$  changes only in the last digit.

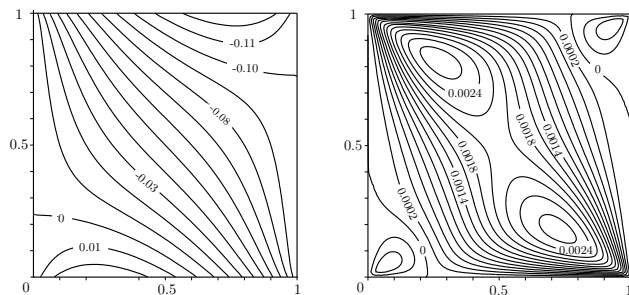


FIG. 9: The isolines of the potential  $\bar{\varphi}(x, y)$  (left) and the streamlines for  $\bar{\psi}(x, y, t)$  at  $t = 200$  ( $\approx 15.6$  s)

In Fig. 9 the tangential velocity at the boundary  $y = 0$  changes its sign at  $x = X_0 \approx 0.2$ . The computations show that the additional vortices in the angles of the domain do not appear if  $X_0 \lesssim 0.1$ . In particular, for  $X = 1$ ,  $Y = 1$ ,  $E_0 = 0.19$  the generation of the rotating flow takes place when  $|\varphi_0| > 0.6$ . It is also interesting to see the differences between the distributions of potentials (*cf.* Figs. 4 and 9).

## VII. DISCUSSION

1. The existence of the discovered EHD rotational flow may be expected since it can be generated by the tangential velocity at the boundaries. Nevertheless we should emphasise once more that a rotational flow appears as the result of the applying of **constant** fields  $\mathbf{E}_{\text{out}}$  and  $\varphi_0$ , as it appears in the experiments [1, 2].

2. The important result of this paper is the obtained in Sect. IV relation between the tangential velocity at the boundary and Reynolds stresses. Our averaged equations (16)–(20) are almost identical to the derived in [3, 4, 5, 6, 7], although we used different boundary conditions (8)–(11). In [3, 4, 5, 6, 7] electrokinetic instability for the solutions corresponding to inhomogeneous conductivity were studied. The Reynolds stresses terms were also derived in these papers, however they had been neglected due to their smallness. In our model (16)–(20) the situation is right the opposite. Reynolds stresses represent the main reason for the appearance of the tangential velocity near the boundaries. One can also see in Appendix A that our averaging method is more detailed than the one given in [3, 4, 5, 6, 7].

3. A full quantitative comparison of our results with the experiments [1, 2] is impossible, since the key information about the values of some crucial parameters (*e.g.* about the thickness of a film) is absent in these papers.

4. The qualitative comparison of our results (Figs. 5, 7, 8) with the flow pictures in [1, 2] shows a good agreement: both in the experiments and in our computations one can observe the appearance of the rotational flow, growing to its stationary state during the time-interval of the order of 2 s. This fact opens the opportunity for a fast switching between the directions of a rotation as has been proposed in [1, 2]. The magnitudes of rotational velocities in our results and in the experiments are similar (around 3 cm/s, at least near the boundaries).

5. In the experiments the flows with one vortex and with two vortices can be observed. Our computations show that only one steady vortex can exist. Our results show (similar to the experiments) that there are two co-rotating vortices in the rectangular film with the ratio of sizes 1:2. However our computations also show that such a flow is not steady, it finally transforms to the flow with single vortex (Fig. 7). However the authors [1, 2] do not mention whether or not the observed flow with two vortices is steady. This contradiction can be resolved provided that the experimental observations correspond to an unsteady flow.

6. The experimental rotating flow [1, 2] appears only for some critical values of the electrical field  $E_0^*$ , which depend on  $\varphi_0^*$ . The authors [1, 2] mistakenly stated that  $E_0^* \varphi_0^* = \text{const}$ . Their graph of this function in two logarithmic scales indeed represents a straight line, however its slope is not  $-1$ . For our model (40)–(44) a rotational flow also appears only for the certain values of parameters. The rough estimation of these parameters follows from (45) (see also the comments to Fig. 9). The rotational flow with one vortex appears when the tangential velocity changes its sign at the point  $x \lesssim 0.1X$ .

7. The experimental speed of the rotation does not depend on the viscosity  $\nu^*$ , while the formula (46) for the tangential velocity gives  $(a/T)\mathcal{R}_3 \sim (\nu^*)^{-3}$ . However for the liquids with different viscosities (the solutions of glycerin in water) the thickness of the films also can be different, while the velocity is  $(a/T)\mathcal{R}_3 \sim (\nu^*)^{-3}h^4$ . We

are unable to compare this formula with the experiments, since the data on a film thickness in [1, 2] are absent.

8. In our model (16)–(20) and in the numerical results (Figs. 4–8) the speed of the rotation decreases towards the center of a film. It looks natural, since the cause of this rotation is the tangential velocity at the boundary (see the boundary conditions (42)). In contrary, the results [1, 2] show that the speed of the rotation increases towards the center of a film. On the basis of this fact the authors of [1, 2] deny electrokinetic effects at the film edges as the possible mechanism that causes the rotation. However one can propose a number of possible explanations for this discrepancy. First, it can be the incompleteness of our mathematical model that does not consider the surface tension and the deviations of the free surfaces of a film from the planes. Second, our mathematical model describes the *averaged* velocity field that differs from the real three-dimensional velocity distribution (see (A17)). Due to the accepted electroneutrality of the mixture (almost everywhere except in the vicinities of the boundaries) the taking into account the three-dimensionality of a flow can produce the decreasing of the rotation for the layers of a film near its boundary. At the same time it is unclear whether the data in [1, 2] represent the average rotation speed or the speed of the rotation of the layer (*e.g.* the free surface) of a film. Third, a more complete mathematical model has to consider the Joule heat that naturally appears in a weakly conductive liquid under a significant electrical current ( $0.2 \text{ mA} \times 20 \text{ V} = 4 \text{ mW}$ ). The resulting nonuniform temperature can cause strong inhomogeneity in viscosity and the permittivity of a solution. We should recall here that the changing of temperature in the interval  $15\text{--}35^\circ\text{C}$  produces the changing of water permittivity  $\varepsilon_r$  in the interval  $81.9\text{--}74.8$  ( $\partial\varepsilon_r/\partial T \approx 0.35$ ). For a strong electrical field it can produce a significant pondermotive force  $(1/2)\nabla\varepsilon(\nabla\varphi)^2$ .

9. Our model of a rotational flow looks more realistic than the heuristic hypothesis of [1, 2] on the changing of the orientations of water molecular dipoles by an external electrical field.

10. The rotating flow in our model is caused by the tangential velocity applied at the boundaries. This velocity has opposite directions at the different parts of the boundary. Therefore it is interesting to study more systematically the vortex flows that appear at various critical values of the applied tangential velocity.

11. Our model (16)–(27) represents only a simplest asymptotic model of the flow near the boundary. There is a serious potential for the development of this theory. Here one should keep in mind that the modelling of EHD processes in micro-scales represents a rather complex problem due to the broad spectrum of various physical phenomena such as electrokinetic effects (electroosmosis, electrophoresis, *etc.*), the effects of diffusion, the chemical reactions both in a solution and on electrodes, the mass-transfer by an electric field, the Joule heat, convection, Taylor-Aris dispersion, *etc.* In particular, it is

unclear whether we can consider the equilibrium Boltzmann concentrations  $c_B \approx 10^{-4} \text{ mol/m}^3$  or we have ions of only one sign near the boundaries.

12. It is especially important to explain the connection between our model and the EDL-theories for strong external electrical fields [19, 26, 27, 28, 29, 30, 31]. In our model the rotating flow is caused by the edge effects at the boundaries  $y = 0, Y$ , where simplified boundary conditions lead to the estimation of the value of  $\mathcal{R} = \mathcal{R}_1(E_0) + \mathcal{R}_3(E_0)$  (43), (46). At the same time this simplified model can be upgraded with the use of contemporary EDL-theories (see also the references on pp. 2, 4). This rather complex task can be undertaken if the industrial applications of the *liquid film motor flows* appear. Here one can go ahead with the full solution of the problem that must include the exact evaluation of  $\mathcal{R}_1(E_0)$  and  $\mathcal{R}_3(E_0)$  and the correction of the assumption  $E = \text{const}$  in (29) (see our remark on p. 5). To achieve such a goal one should describe an interface flow more precisely, which is possible only with the use of EDL-theories. In general, the creation of a full industrial level model requires to reconsider or upgrade all results of Sect. IV.

13. In practical applications the *liquid film motor flows* can be used for the micromixing in microfluidic devices.

14. The general significance of our results for the further developments of microhydrodynamics may consist in the reevaluation of the role of the considered classical effects in the micro- and nano-scale processes.

### Acknowledgments

This research is partially supported by EPSRC (research grants GR/S96616/01, EP/D055261/1, and EP/D035635/1), by the Russian Ministry of Education (programme ‘Development of the research potential of the high school’, grants 2.1.1/6095 and 2.1.1/554), and by Russian Foundation for Basic Research (grants 07-01-00389, 08-01-00895, and 07-01-92213 NCNIL). The authors are grateful to the Department of Mathematics of the University of York for the providing of excellent conditions for this research.

### APPENDIX A: THE AVERAGING PROCEDURE

The averaging of (1), (3)–(6), that takes into account the boundary conditions (8)–(11), gives the exact but not closed system of equations

$$\begin{aligned} \delta^2(\partial_t \bar{\mathbf{u}} + \bar{\mathbf{u}} \cdot \nabla_0 \bar{\mathbf{u}}) + \delta^2 \text{div}_0(\overline{\tilde{\mathbf{u}} \otimes \tilde{\mathbf{u}}}) = \\ = -\delta^2 \nabla_0 \bar{p} + \delta^2 \nu \Delta_0 \bar{\mathbf{u}} - \bar{q} \nabla_0 \bar{\varphi} - \overline{\tilde{q} \nabla_0 \tilde{\varphi}}, \end{aligned} \quad (\text{A1})$$

$$\text{div}_0 \bar{\mathbf{u}} = 0, \quad (\text{A2})$$

$$\varepsilon \Delta_0 \bar{\varphi} = -\bar{q}, \quad (\text{A3})$$

$$\partial_t \bar{c}_k + \bar{\mathbf{u}} \cdot \nabla_0 \bar{c}_k + \operatorname{div}_0(\overline{\bar{\mathbf{u}}\bar{c}_k}) + D_k \operatorname{div}_0 \bar{\mathbf{i}}_k = 0, \quad (\text{A4})$$

$$\bar{\mathbf{i}}_k = -D_k(\nabla_0 \bar{c}_k + e_k \gamma \bar{c}_k \nabla_0 \bar{\varphi} + e_k \gamma \overline{\bar{c}_k \nabla_0 \bar{\varphi}}). \quad (\text{A5})$$

In order to obtain the closed system with the precision  $O(\delta^4)$  we use the decompositions (15) to calculate the terms

$$\overline{\bar{\mathbf{u}} \otimes \bar{\mathbf{u}}} = \overline{\bar{\mathbf{u}}^0 \otimes \bar{\mathbf{u}}^0} + O(\delta^2), \quad (\text{A6})$$

$$\overline{\bar{q} \nabla_0 \bar{\varphi}} = \overline{(\bar{q}^0 + \delta^2 \bar{q}^1) \nabla_0 (\bar{\varphi}^0 + \delta^2 \bar{\varphi}^1)} + O(\delta^4), \quad (\text{A7})$$

$$\overline{\bar{\mathbf{u}} \bar{c}_k} = \overline{(\bar{\mathbf{u}}^0 + \delta^2 \bar{\mathbf{u}}^1)(\bar{c}_k^0 + \delta^2 \bar{c}_k^1)} + O(\delta^4), \quad (\text{A8})$$

$$\overline{\bar{c}_k \nabla_0 \bar{\varphi}} = \overline{(\bar{c}_k^0 + \delta^2 \bar{c}_k^1) \nabla_0 (\bar{\varphi}^0 + \delta^2 \bar{\varphi}^1)} + O(\delta^4). \quad (\text{A9})$$

For the main terms in (15) equations (2), (4)–(6) and condition (10) yield

$$(\bar{q}^0 + \bar{q}^0) \partial_z \bar{\varphi}^0 = 0, \quad \bar{q}^0 + \bar{q}^0 = \sum_k e_k (\bar{c}_k^0 + \bar{c}_k^0), \quad (\text{A10})$$

$$\partial_z \bar{I}_k^0 = 0, \quad \bar{I}_k^0 + \bar{I}_k^0 = \partial_z \bar{c}_k^0 + e_k \gamma (\bar{c}_k^0 + \bar{c}_k^0) \partial_z \bar{\varphi}^0. \quad (\text{A11})$$

$$(\bar{I}_k^0 + \bar{I}_k^0)|_{z=\pm 1} = 0.$$

Equations (A10), (A11) give  $\partial_z \bar{\varphi}^0 = 0$ ,  $\partial_z \bar{I}_k^0 = 0$ ,  $\bar{I}_k^0 = \partial_z \bar{c}_k^0$ . It is clear that if  $\partial_z \bar{f} = 0$ , then  $\bar{f} = 0$  and  $f = \bar{f}$ . Hence

$$\bar{\varphi}^0 = 0, \quad \bar{c}_k^0 = 0, \quad \bar{q}^0 = 0, \quad (\text{A12})$$

$$\varphi^0 = \bar{\varphi}^0, \quad c_k^0 = \bar{c}_k^0, \quad q^0 = \bar{q}^0.$$

The use of (A12) transforms the expressions (A7)–(A9) to the form

$$\overline{\bar{q} \nabla_0 \bar{\varphi}} = O(\delta^4), \quad (\text{A13})$$

$$\overline{\bar{\mathbf{u}} \bar{c}_k} = \delta^2 \overline{\bar{\mathbf{u}}^0 \bar{c}_k^1} + O(\delta^4), \quad \overline{\bar{c}_k \nabla_0 \bar{\varphi}} = O(\delta^4).$$

From (1), (A12) we obtain the equation for  $\bar{\mathbf{u}}^0$

$$\nu \partial_{zz} \bar{\mathbf{u}}^0 - \bar{q}^0 \nabla_0 \bar{\varphi}^0 = 0,$$

which is required for the calculation of (A6) with the precision  $O(\delta^2)$ . In particular it means that we can make the replacements  $\bar{q} = \bar{q}^0 + O(\delta^2)$ ,  $\bar{\varphi} = \bar{\varphi}^0 + O(\delta^2)$  and  $\bar{w}_0, \bar{\mathbf{u}}_0$  can be found from the equations

$$\nu \partial_{zz} \bar{\mathbf{u}}^0 - \bar{q} \nabla_0 \bar{\varphi} = 0, \quad (\text{A14})$$

$$\operatorname{div}_0(\bar{\mathbf{u}}^0 + \bar{\mathbf{u}}^0) + \partial_z \bar{w}^0 = 0, \quad (\text{A15})$$

with the boundary condition

$$\bar{w}^0 + \bar{w}^0 = 0, \quad z = \pm 1. \quad (\text{A16})$$

We assume that  $\bar{w}^0 = 0$ . The integration of (A14)–(A16) yields

$$\bar{\mathbf{u}}^0 = g'(z) \mathbf{U}, \quad \bar{w}^0 = -g(z) \operatorname{div}_0 \mathbf{U}, \quad \nu \mathbf{U} = \bar{q} \nabla_0 \bar{\varphi}, \quad (\text{A17})$$

$$\operatorname{div}_0 \bar{\mathbf{u}}^0 = 0, \quad g(z) = \frac{1}{6}(z^3 - z), \quad \overline{g(z)} = 0, \quad \overline{g'(z)} = 0,$$

where we have used the notation (20) for  $\mathbf{U}$ .

One can notice that we do not require  $\bar{\mathbf{u}}^0$  to satisfy the boundary condition (9). This condition is required only for  $\bar{\mathbf{u}}$ . The equality  $\partial_z \bar{\mathbf{u}}^0 = 0$  at  $z = \pm 1$  leads to  $\mathbf{U} = 0$  that is not true. In the exact problem one should consider a boundary-layer solution at  $z = \pm 1$  and assume the absence of the charge ( $\bar{q} = 0$ ) at the boundary. In the opposite case the action of a tangential to the boundary external field creates the stresses related to Maxwell's electromagnetic stress tensor.

The use of (A17) gives the expression for (A6)

$$\overline{\bar{\mathbf{u}} \otimes \bar{\mathbf{u}}} = \overline{g'^2(z)} (\mathbf{U} \otimes \mathbf{U}) + O(\delta^2), \quad \overline{g'^2(z)} = \frac{1}{45}. \quad (\text{A18})$$

The calculation of  $\overline{\bar{\mathbf{u}} \bar{c}_k}$  is based on the next approximation for the equations (4)–(6)

$$\partial_t c_k^0 + \mathbf{u}^0 \cdot \nabla_0 c_k^0 + w^0 \partial_z c_k^0 + \operatorname{div}_0 \mathbf{i}_k^0 + \partial_z I_k^1 = 0,$$

$$\mathbf{i}_k^0 = -D_k \left( \nabla_0 c_k^0 + e_k \gamma c_k^0 \nabla_0 \varphi^0 \right),$$

$$I_k^1 = -D_k \left( \partial_z c_k^1 + e_k \gamma (c_k^1 \partial_z \varphi^0 + c_k^0 \partial_z \varphi^1) \right),$$

$$\varepsilon (\Delta_0 \varphi^0 + \partial_{zz} \varphi^1) = -q^0$$

or taking in account (A12)

$$\partial_t \bar{c}_k^0 + (\bar{\mathbf{u}}^0 + \bar{\mathbf{u}}^0) \cdot \nabla_0 \bar{c}_k^0 + \operatorname{div}_0 \mathbf{i}_k^0 + \partial_z I_k^1 = 0, \quad (\text{A19})$$

$$\mathbf{i}_k^0 = -D_k \left( \nabla_0 \bar{c}_k^0 + e_k \gamma \bar{c}_k^0 \nabla_0 \bar{\varphi}^0 \right),$$

$$I_k^1 = -D_k \left( \partial_z \bar{c}_k^1 + e_k \gamma \bar{c}_k^0 \partial_z \bar{\varphi}^1 \right),$$

$$\varepsilon (\Delta_0 \bar{\varphi}^0 + \partial_{zz} \bar{\varphi}^1) = -\bar{q}^0.$$

The last equation shows that  $\partial_{zz} \bar{\varphi}^1$  does not depend on  $z$ , so to find  $\bar{c}_k^1$  we obtain the equation

$$\bar{\mathbf{u}}^0 \cdot \nabla_0 \bar{c}_k^0 - D_k \partial_{zz} \bar{c}_k^1 = 0 \quad (\text{A20})$$

with the boundary conditions that follow from (10)

$$\partial_z \widetilde{c}_k^1|_{z=\pm 1} = 0.$$

For the calculation of  $\overline{\mathbf{u}\widetilde{c}_k}$  one can take  $\overline{c}_k = \overline{c}_k^0 + O(\delta^2)$  in (A20), since the required precision for (A8) is  $O(\delta^2)$ . It allows us to integrate the equation (A20)

$$D_k \widetilde{c}_k^1 = (g_0(z) - \overline{g_0(z)}) \mathbf{U} \cdot \nabla_0 \overline{c}_k, \quad g_0(z) = \frac{z^2}{12} \left( \frac{1}{2} z^2 - 1 \right).$$

Finally we obtain

$$\overline{\mathbf{u}^0 \widetilde{c}_k^1} = -\alpha_k \mathbf{U} (\mathbf{U} \cdot \nabla_0 \overline{c}_k), \quad (\text{A21})$$

$$\alpha_k = -\frac{1}{D_k} \left( \overline{g'(z)(g_0(z) - \overline{g_0(z)})} \right) = \frac{4}{945 D_k}.$$

## APPENDIX B

Let us show that in the case (29) equations (16) can be integrated. The use (36) and (20) gives the velocity component  $\overline{u}$

$$\frac{\beta}{\nu^2} E \partial_y (\overline{q}^2 \partial_y \Phi) = -\delta^2 \partial_x p + \nu \delta^2 \partial_{yy} \overline{u} - \overline{q} E. \quad (\text{B1})$$

Taking in account that  $\overline{q}$ ,  $\Phi$  and  $\overline{u}$  depend only on  $y$  we get

$$-\delta^2 p = \left\{ \frac{\beta}{\nu^2} E \partial_y (\overline{q}^2 \partial_y \Phi) - \nu \delta^2 \partial_{yy} \overline{u} + \overline{q} E \right\} x + H(y).$$

Its substitution into the equation (16) for  $w$  shows that  $p$  depends on  $y$  only

$$\frac{\beta}{\nu^2} \partial_y (\overline{q} \partial_y \Phi)^2 + \overline{q} \partial_y \Phi = H'(y).$$

It follows that the expression in braces is vanishing and (B1) gives (37).

## APPENDIX C

Let us consider the case when the values of all diffusion coefficients are the same ( $D_k \equiv D$ ). The multiplying of (A4) by  $e_k$  and combining the results yield

$$\frac{d\overline{q}}{dt} + \text{div}_0(\overline{\mathbf{u}\overline{q}}) - D \text{div}_0(\nabla_0 \overline{q} + \sigma \nabla_0 \overline{\varphi}) = 0,$$

where  $\sigma = D \sum_k e_k^2 \gamma \overline{c}_k$  is the conductivity of a mixture; we have also taken (A21) into account. By virtue of (A21) the electroneutrality  $\overline{q} = 0$  leads to  $\widetilde{q} = 0$  everywhere except the boundaries. Hence, in the case  $\overline{c}_k = c_B$  (see (31)) we arrive to the equation (41).

Recall that the requirement of the equality of all diffusion coefficients represents a strong restriction. In particular, the difference between the diffusion coefficients leads to the participation of the term  $\overline{\mathbf{u}\overline{q}}$  (linked to the Taylor–Aris dispersion [3, 4, 5, 6, 7]) into the electrokinetic instabilities.

- 
- [1] A. Amjadi, R. Shirsavar, N. Hamedani Radja, and M. R. Ejtehad, e-print arXiv:cond-mat/0805.0490v2 (2008).  
[2] R. Shirsavar, A. Amjadi, N. Hamedani Radja, M. D. Nirya, M. Reza Rahimi Tabar, and M. R. Ejtehad, e-print arXiv:cond-mat/0605029v1 (2006).  
[3] M. H. Oddy and J. G. Santiago, *Phys. Fluids*. **17**, 064108 (2005).  
[4] B. D. Storey, B. S. Tilley, Hao Lin, and J. G. Santiago, *Phys. Fluids*. **17**, 018103 (2005).  
[5] C.-H. Chen, H. Lin, Sanjiva K. Lele and J. G. Santiago, *J. Fluid Mech.* **524** (2005).  
[6] H. Lin, B. D. Storey and J. G. Santiago, *J. Fluid Mech.* **608** (2008).  
[7] H. Lin, B. D. Storey, M. H. Oddy, Chuan-Hua Chen, and J. G. Santiago, *Phys. Fluids*. **16**, 6 (2004).  
[8] J. C. Baygents and F. Baldessari, *Phys. Fluids*. **10**, 1 (1998).  
[9] H.-K. Yeoh, Q. Xu, O. A. Basaran, *Phys. Fluids*. **19**, 11 (2007).  
[10] B. S. Tilley, P. G. Petropoulos, and D. T. Papageorgiou, *Phys. Fluids*. **13**, 12 (2001).  
[11] D. Tseluiko, M. G. Blyth, D. T. Papageorgiou, and J.-M. Vanden-Broeck, *Phys. Fluids*. **20**, 4 (2008).  
[12] N. A. Mortensen, L. H. Olesen, L. Belmon, and H. Bruus, *Phys. Rev. E*, **71**, 056306 (2005).  
[13] K. T. Chu and M. Z. Bazant, *J. Colloid and Interface Science*. **315** (2007).  
[14] Z. G. Chiragwandi, O. Nur, M. Willander, and I. Panas, *Appl. Phys. Lett.* **87**, 153109 (2005).  
[15] V. B. Deyirmenjian, Z. A. Daya, and S. W. Morris, e-print arXiv:patt-sol/9703001v1 (1997).  
[16] J. R. Melcher and G. I. Taylor, *Annu. Rev. Fluid Mech.* **1**, 111 (1969).  
[17] R. M. Ehrlich and J. R. Melcher, *Phys. Fluids*. **25**, 10 (1982).  
[18] D. A. Saville, *Annu. Rev. Fluid Mech.* **29** (1997).  
[19] B. Zaltzman, I. Rubinstein, *J. Fluid Mech.* **579** (2007).  
[20] M. S. Kilic and M. Z. Bazant, e-print arXiv:0712.0453v1 (2007).  
[21] M. Z. Bazant, K. Thornton, and A. Ajdari, *Phys. Rev. E*. **70**, 021506 (2004).  
[22] A. Ajdari, *Phys. Rev. E* **53**, 4996 (1996).  
[23] A. Ajdari, *Phys. Rev. Lett.* **75**, 755 (1995).  
[24] A. Ajdari, *Phys. Rev. E* **65**, 016301 (2001).  
[25] J. G. Santiago, *Anal. Chem.* **73** (2001).  
[26] M. S. Kilic, M. Z. Bazant, and A. Ajdari, *Phys. Rev. E* **75**, 021502 (2007).  
[27] B. D. Storey, L. R. Edwards, M. S. Kilic, and

- M. Z. Bazant, Phys. Rev. E **77**, 036317 (2008).
- [28] M. S. Kilic, M. Z. Bazant, and A. Ajdari, Phys. Rev. E **75**, 021503 (2007).
- [29] K. T. Chu and M. Z. Bazant, e-print arXiv:physics/0406076v1 (2004).
- [30] M. Z. Bazant, K. T. Chu, and B. J. Bayly, e-print arXiv:physics/0406075v1 (2004).
- [31] S. S. Dukhin, R. Zimmermann, and C. Werner, Colloids and Surfaces A: Physicochemical and Engineering Aspects. **195** 1–3 (2001).
- [32] T. M. Squires and S. R. Quake, Rev. Mod. Phys. **77**, 3 (2005).
- [33] H. A. Stone, A. D. Stroock, and A. Ajdari, Annu. Rev. Fluid Mech. **36** (2004).
- [34] D. Erickson and D. Li, Langmuir. **19** (2003).
- [35] S. V. Ermakov, S. C. Jacobson, and J. M. Ramsey, Anal. Chem. **70**, 21 (1998).
- [36] S. V. Ermakov, S. C. Jacobson, and J. M. Ramsey, Anal. Chem. **72**, 15 (2000).
- [37] Y. Hu, C. Werner, and D. Li, Anal. Chem. **75** (2003).
- [38] S. Pennathur and J. G. Santiago, Anal. Chem. **77**, 21 (2005).
- [39] J. D. Posner and J. G. Santiago, J. Fluid Mech. **555** (2006).
- [40] D. Kaniansky, M. Masár, R. Bodor, M. Zuborova, E. Ölvecká, M. Jöhnck, and B. Stanislawski, Electrophoresis. **24**, 12–13 (2003).
- [41] R. Bharadwaj, J. G. Santiago, and B. Mohammadi, Electrophoresis. **23** (2002).
- [42] J. I. Molho, A. E. Herr, B. P. Mosier, J. G. Santiago, and Th. W. Kenny, Anal. Chem. **73** (2001).
- [43] C. Jen, C. Wu, Y. Lin, and C. Wu, Lab Chip. **3** (2003).
- [44] T. J. Johnson, D. Ross, and L. E. Locascio, Anal. Chem. **74** (2002).
- [45] M. H. Oddy, J. C. Mikkelsen, and J. G. Santiago, Anal. Chem. **73** (2001).
- [46] D. Laser and J. G. Santiago, J. of Micromechanics and Microengineering. **14**, 6 (2004).
- [47] J. D. Jackson, *Classical Electrodynamics* (Wiley, New York, 1963).
- [48] L. D. Landau and E. M. Lifshitz, *Electrodynamics of Continuous Media* (Pergamon Press, Oxford, 1985).
- [49] A. M. Ilin, *Matching of asymptotic expansions of solutions of boundary value problems* (Providence, R. I.: American Mathematical Society, 1992).
- [50] A. Chorin, J. Comput. Phys. **2** (1967).
- [51] R. Rannacher, in ‘Navier-Stokes Equations: Theory and Numerical Methods’ (R. Rautmann, et al., eds.). Proc. Oberwolfach Conf. 1991. (Springer, 1992).
- [52] F. Hecht, O. Pironneau, A. Le Hyaric, and K. Ohtsuka, FreeFem++. Manual. <http://www.freefem.org/ff++>.
- [53] In the case of the insulator-conductor, the interface condition (21) correspond to the surface charge density  $\pm \varepsilon_{\text{out}} |\mathbf{E}_{\text{out}}| \cos \alpha$  on the plates of the capacitor  $y = 0, Y$ . One can also prescribe different boundary condition, for example  $\varphi = \pm \varphi_{\text{out}}|_{y=0, Y}$ .